scientific reports

OPEN

Long distance entanglement and high-dimensional quantum teleportation in the Fermi–Hubbard model

Sanaa Abaach[1,3], Zakaria Mzaouali[2,3]✉ & Morad El Baz[1,3]

The long distance entanglement in finite size open Fermi–Hubbard chains, together with the end-to-end quantum teleportation are investigated. We show the peculiarity of the ground state of the Fermi–Hubbard model to support maximum long distance entanglement, which allows it to operate as a quantum resource for high fidelity long distance quantum teleportation. We determine the physical properties and conditions for creating scalable long distance entanglement and analyze its stability under the effect of the Coulomb interaction and the hopping amplitude. Furthermore, we show that the choice of the measurement basis in the protocol can drastically affect the fidelity of quantum teleportation and we argue that perfect information transfer can be attained by choosing an adequate basis reflecting the salient properties of the quantum channel, i.e. Hubbard projective measurements.

The second quantum revolution is driven by the revolutionary ideas of exploiting the inherent quantum properties of atomic systems in order to achieve a quantum advantage over classical methods in the manipulation of information[1,2]. One of the facets of quantum information processing is quantum teleportation, which is a protocol offering the possibility of transferring an unknown quantum state using pre-existing entanglement and a classical information channel[3]. The introduction of the protocol in 1993 by Bennett et al., and its experimental realization in 1997 by the group led by Zeilinger[4] shifted the concept of teleportation from being fictional to a physical reality[5].

Quantum teleportation rely primarily on the entanglement shared between the sending and receiving party through the quantum channel[6]. Therefore, the creation and distribution of entanglement in physical platforms is crucial in the success and implementation of quantum teleportation protocols[7]. In this context, a variety of one-dimensional quantum spin chains are known for their entangled ground states and have been intensively investigated as faithful architectures for quantum information processing[8–15] and notably as reliable quantum channels for teleportation protocols[16–26]. Nevertheless, in most one-dimensional quantum spin chain systems with short-range interactions, the entanglement vanishes for distances larger than two neighboring sites[27–29], which makes them inconceivable platforms for long distance teleportation.

Accordingly, efforts have been devoted to produce some mechanisms able to create sizable entanglement between distant but not necessarily directly interacting constituents. An early initiative was the introduction of the concept of localizable entanglement, which defines the concentrated entanglement on an arbitrary distant pair by implementing optimal local measurements onto the rest of the system[7]. Such kind of entanglement is defined as long distance entanglement (LDE).

A promising candidate for creating LDE is the gapped one-dimensional antiferromagnetic spin chain. In this regard, Venuti et al.[7] have proposed a scheme for creating LDE in spin-$\frac{1}{2}$ and spin-1 chains, showing that this property appears only for given values of a specific microscopic parameter, which doesn't coincide with known quantum critical points. Later, schemes have been suggested for generating LDE in *XX* spin chains[30,31], in many-body atomic and optical systems[32], in Motzkin and Fredkin spin chains[33], and in antiferromagnetic *XXZ* spin chain with alternating interactions[34] as well. Additionally, it has been shown that robust temporally shaped control pulses for producing LDE can be derived in disordered spin chains[35] and that LDE can be enhanced for spin chains with dissipative processes through global measurements[36]. Recently, an experimental implementation of LDE has been realised between unpaired spins in antiferromagnetic spin-$\frac{1}{2}$ chains in a bulk material[37].

[1]ESMaR, Faculty of Sciences, Mohammed V University in Rabat, Rabat, Morocco. [2]Institute of Theoretical and Applied Informatics, Polish Academy of Sciences, Bałtycka 5, 44-100 Gliwice, Poland. [3]These authors contributed equally: Sanaa Abaach, Zakaria Mzaouali and Morad El Baz. ✉email: zmzaouali@iitis.pl

As a consequence of the appealing LDE generation property, it has been recently demonstrated that LDE allows for robust qubit teleportation and state transfer with high fidelity, across sufficiently long distances in finite size spin chains[30,38].

So far, investigating the generation of LDE has been limited to qubit spin chains. However, increasing the dimensionality and the complexity of the system has been shown to enhance the capacity of the quantum communication channel[39,40], and improves the robustness against eavesdropping attacks[41,42]. Additionally, high-dimensional entangled states can be used for quantum state transfer of ever-increasing complexity[43–45]. Similarly, the majority of quantum teleportation experiments, were limited to two-dimensional subspaces (qubits), including quantum dot spin qubits[46]. Recently, quantum teleportation has been achieved in high-dimensional quantum photonic systems[47,48]. An alternative for photonic platforms, which causes the propagation losses of light, are quantum dots as they are the most scalable and time coherent architectures dedicated for quantum simulation and implementing quantum information tasks in the form of communication and computing[49]. Recently, it has been shown that quantum dot systems described by the ground state of the Hubbard model are a promising entanglement resource for performing quantum teleportation of four-dimensional states[50].

The main goal of this paper is to analyze long distance quantum teleportation in quantum dots described by the ground state of the one-dimensional Fermi–Hubbard model. We start in "The model and the teleportation protocol" section by introducing the general form of the Fermi–Hubbard Hamiltonian, and presenting the generalized standard teleportation protocol with an arbitrary mixed state resource in higher dimensions, as well as the fidelity of quantum teleportation. Moreover, we define the lower bound of concurrence for measuring the end-to-end entanglement in bipartite high dimensional states. The aforementioned framework allows us in "Long distance entanglement and fidelity enhancement" section to discuss two schemes for creating end-to-end entanglement in an open Fermi–Hubbard chain, one by implementing bonds of alternating strengths defined in[7] and the other by alternating hopping amplitudes. Additionally, we show the important interplay between the choice of the measurement basis in the protocol and achieving perfect quantum teleportation with unit fidelity. Finally, in "Conclusion" section we summarize our core results and conclusions.

The model and the teleportation protocol

The Fermi–Hubbard model.
The Fermi–Hubbard (FH) model describes moving fermions with spin in a lattice[51]. In one-dimensional settings, it is given by

$$H = -t \sum_{i,\sigma} \left(c_{i,\sigma}^\dagger c_{i+1,\sigma} + c_{i+1,\sigma}^\dagger c_{i,\sigma} \right) + u \sum_i n_{i,\uparrow} n_{i,\downarrow}, \tag{1}$$

where $c_{i,\sigma}^\dagger$ and $c_{i,\sigma}$ are, respectively, the creation and annihilation operators that describe the tunneling of electrons between the neighboring sites. t is the hopping amplitude and $\sigma = \{\uparrow, \downarrow\}$ indicates spin-up or spin down electron, whereas u is the on-site electron-electron Coulomb interaction. We assume that only the s-orbital is allowed to the electrons in each site, so that, each site is able to hold up to two electrons with opposite spins as stated by the Pauli exclusion principle. Thereby, electrons have four possibilities in occupying a single site: $|0\rangle$, $|\uparrow\rangle, |\downarrow\rangle$ and $|\uparrow\downarrow\rangle$. When the Coulomb interaction u is strong enough, the tunneling of electrons between the sites t is blocked leading to the quantum confinement effect in the FH system. This physical picture is analogous to the formation of potential barriers between the sites that prohibits electrons to tunnel outside. Experimentally, the creation of such barriers is made by modulating potentials, using gate electrodes, in order to control the tunneling of electrons between the sites that are simulated using semiconductor quantum dots[52].

The Fermi–Hubbard Hamiltonian, Eq. (1), is a prototype model to describe and investigate the properties of quantum systems, such as: the metal-insulator transition, ferromagnetism, ferrimagnetism, and antiferromagnetism. As well as, superconductivity and Tomonaga-Luttinger liquid[53]. Furthermore, the intersection between quantum information theory and condensed matter physics has been a subject of interest in fermionic models. In particular, it has been shown that entanglement plays a role in the identification of the phases of matter present in the Hubbard model[54–60]. At the experimental level, quantum simulation of the Hubbard model using ultra cold atoms in optical lattices have been successful in observing and validating the theoretical results of strongly correlated Fermi gases[61]. In the following, we will consider the dimensionless quantity $U = u/t$ as the main parameter in the model, Eq. (1).

Quantum teleportation with d-dimensional channels.
The standard quantum teleportation protocol with Bell states resources resource is an example of a noiseless channel. It allows the transfer of information from a sender A to a receiver B using Bell measurements and Pauli rotations. In general, quantum teleportation uses entangled mixed states as a resource, which renders the protocol equivalent to information transfer via a noisy channel[62]. To teleport information encoded in a $d-$dimensional unknown state $|\Psi\rangle = \sum_{j=0}^{d-1} \alpha_j |j\rangle$, where $\alpha_i \in \mathbb{C}$, the teleportation protocol have to operate using an entangled two qudit $(d \times d)$ state as a state resource. Hence, the teleportation protocol is constructed and formulated basing on the maximally entangled Bell state

$$|\psi^+\rangle = \frac{1}{\sqrt{d}} \sum_j |j\rangle |j\rangle, \tag{2}$$

and the set of unitary generators

$$U^{nm} = \sum_k e^{2\pi i k n/d} |k\rangle \langle k \oplus m|, \tag{3}$$

that act on the first subsystem, where $\oplus$ denotes the addition modulo d. Interestingly, it has been shown that the output state is equivalent to the state produced by a depolarizing channel[62], given by

$$\epsilon(\varrho) = \sum_{nm} \text{Tr}[E^{nm}\chi]U^{n(-m)}\varrho(U^{n(-m)})^{\dagger}, \tag{4}$$

where χ denotes the quantum state resource or the shared entangled mixed state between the sender and the receiver in a teleportation protocol, and E^{nm} are the set of maximally entangled Bell state projectors given by

$$E^{nm} = U^{nm}|\psi^+\rangle\langle\psi^+|(U^{nm})^{\dagger}, \tag{5}$$

with $n, m = 0, 1, \ldots, d-1$ and $\varrho = |\Psi\rangle\langle\Psi|$.

In the Fermi–Hubbard chain, a site i and a site j, for $i \neq j$, are respectively assumed to be the sender and the receiver systems in the quantum teleportation scheme. The state ρ_{ij} describing the couple of sites (sender and receiver) represents the entangled mixed state resource in the teleportation protocol. A four-dimensional unknown state

$$|\Psi\rangle = \alpha_0|0\rangle + \alpha_1|1\rangle + \alpha_2|2\rangle + \alpha_3|3\rangle, \tag{6}$$

is considered as the state to be teleported using the following depolarizing channel

$$\epsilon_{ij}(|\Psi\rangle\langle\Psi|) = \sum_{n,m=0}^{3} \text{Tr}[E^{nm}\rho_{ij}]U^{n(-m)}|\Psi\rangle\langle\Psi|(U^{n(-m)})^{\dagger}, \tag{7}$$

where the projectors E^{nm} are constructed by means of the four-dimensional maximally entangled Bell state

$$|\psi^{\dagger}\rangle = \frac{1}{2}(|00\rangle + |11\rangle + |22\rangle + |33\rangle). \tag{8}$$

The standard quantum teleportation channel being noisy hinders the perfect information transfer using a general $(d \times d)$ bipartite state as a resource, instead of $|\psi^+\rangle$. Accordingly, measuring how well the output state $\epsilon(\varrho)$ and the input state ϱ are similar in a quantum teleportation scheme is quantified through the concept of the fidelity[63]. It is defined as

$$\mathscr{F} = \text{Tr}(\varrho\epsilon(\varrho)). \tag{9}$$

For orthogonal states the fidelity is zero, while it reaches a unit value for identical states. Correspondingly, the efficiency and the quality of a quantum channel in teleporting an unknown state is presented in terms of the average fidelity $\overline{\mathscr{F}}$ over all possible input states, which can be written as

$$\overline{\mathscr{F}} = \frac{d}{d+1}f + \frac{1}{d+1}, \tag{10}$$

where

$$f = \langle\psi^+|\chi|\psi^+\rangle, \tag{11}$$

and χ is the quantum state resource. $\overline{\mathscr{F}}(\epsilon)$ is proven to be the maximal achievable teleportation fidelity in the standard teleportation protocol, where f is the fully entangled fraction[64–66]. Indeed, one requires the average fidelity to be larger than $\frac{2}{d+1}$ to outperform the purely classical communication protocols. Hence, for a two-qudit state χ, as a resource to be useful for quantum teleportation, the fully entangled fraction f needs to satisfy $f > \frac{1}{d}$.

The key ingredient for the success of the teleportation protocol is the entanglement shared between the sender and receiver, that is actually the quantum state resource χ. Therefore, quantifying the entanglement in quantum systems is crucial in order to evaluate and improve the fidelity of the quantum teleportation protocol. Accessing the amount of entanglement in many-body quantum systems is a challenging task and exact formulas are known only for some configurations, e.g. qubit-qubit, and qubit-qutrit systems[67]. In[68] the authors introduced an analytical lower bound of concurrence as an effective evaluation of entanglement for arbitrary bipartite quantum states by decomposing the joint Hilbert space into many $2 \otimes 2$ dimensional subspaces and without any optimization procedure. This lower bound was recently extended to arbitrary N-partite states[69,70] that provides better estimates of the entanglement in some states comparted to the usual separability criteria.

For an arbitrary mixed state in $d \times d$ dimension, the concurrence $C(\rho_{ij})$[68] satisfies,

$$\tau_2(\rho_{ij}) = \frac{d}{2(d-1)} \sum_{\alpha}^{\frac{d(d-1)}{2}} \sum_{\beta}^{\frac{d(d-1)}{2}} C_{\alpha\beta}^2 \leq C^2(\rho_{ij}), \tag{12}$$

where,

$$C_{\alpha\beta} = max\{0, \lambda_{\alpha\beta}^{(1)} - \lambda_{\alpha\beta}^{(2)} - \lambda_{\alpha\beta}^{(3)} - \lambda_{\alpha\beta}^{(4)}\}. \tag{13}$$

In our case, ρ_{ij} is the pairwise density matrix of the ground state of the Fermi–Hubbard model, Eq. (1), with $(i < j)$. $\lambda_{\alpha\beta}^{(a)}$ are the square roots of the non-zero eigenvalues of the non-Hermitian matrix $\rho_{ij}\tilde{\rho}_{(ij)\alpha\beta}$ such that $\lambda_{\alpha\beta}^{(a)} > \lambda_{\alpha\beta}^{(a+1)}$ for $1 \leq a \leq 3$ and

$$\tilde{\rho}_{(ij)\alpha\beta} = (G_\alpha \otimes G_\beta)\rho_{ij}^*(G_\alpha \otimes G_\beta). \tag{14}$$

Here, G_α is the αth element of the group $SO(d)$.

In the following, using QuSpin[71,72] and QuTiP[73,74], we calculate by numerical diagonalization the ground state of the Fermi–Hubbard model, Eq. (1), in order to exploit it as a resource for teleporting an unknown four-dimensional state $|\Psi\rangle = \frac{1}{N}(\alpha_0|0\rangle + \alpha_1|1\rangle + \alpha_2|2\rangle + \alpha_3|3\rangle)$, where $\alpha_i \in \mathbb{C}$ and N is the normalization constant. Figure S1 in the supplementary materials shows the fidelity $\mathscr{F}$, Eq. (9), as a function of the coefficient α_0, where the state to be teleported is $|\Psi\rangle = \frac{1}{\sqrt{\alpha_0^2+3}}(\alpha_0|0\rangle + |1\rangle + |2\rangle + |3\rangle)$, $\forall \alpha_0 \in \mathbb{R}$. We report that (c.f Figure S1 in supplementary material) $\mathscr{F}$ starts with a small value at $\alpha_0 = 0$. Then as α_0 tends to 1, $\mathscr{F}$ attains a maximum value and decays asymptotically as α_0 continue to increase ($\alpha_0 > 1$). Such behavior indicates that the four dimensional teleportation protocol performance depends essentially on the type of the state to be teleported. Indeed, when $\alpha_0 = 0$ or $\alpha_0 > 1$, the state $|\Psi\rangle$ could be considered respectively as a qutrit state $|\Psi\rangle = \frac{1}{\sqrt{3}}(|1\rangle + |2\rangle + |3\rangle)$ or a qubit state $|\Psi\rangle \simeq |0\rangle$. For both types the quantum teleportation fidelity (c.f Figure S1 in supplementary material) reveals small values in contrast to the quadrit state type, with $\alpha_0 = 1$, where a maximum value is achieved. This implies that the efficient performance of the four dimensional teleportation channel, Eq. (4) necessitates a quadrit input state with $\alpha_i \neq 0$. For this reason, in order to study the behavior of the channel's fidelity, Eq. (9), under the effect of the Coulomb interaction u and the hopping amplitude t, we consider in the following $\alpha_i = \frac{1}{2}$, with $i = 0, 1, 2, 3$.

Figure 1a depicts the end-to-end entanglement quantified using the lower bound concurrence, Eq. (13), in the ground state of the Fermi–Hubbard chain, Eq. (1), for several system sizes. We report that long distance entanglement manifests weakly only for the chain size of $L = 4$, which reflects in the behaviour of the end-to-end fidelity of the quantum teleportation represented in Fig. 1b for the same model parameters. The fidelity shows no quantum advantage as it is below the value of $\frac{2}{5} = 0.4$, which is the upper limit for the classical threshold. In the following, we discuss how to generate long distance entanglement in the Fermi–Hubbard model by manipulating the nature of interactions between the sites, in order to demonstrate a quantum advantage in the quantum teleportation fidelity.

Long distance entanglement and fidelity enhancement

Consider a chain consisting of L sites. In order to create localizable entanglement between the ends of the chain, the interaction between the block of spins, separating the ends of the chains, must be weak with the first and last sites. The localizable entanglement offer a solid framework to exploit quantum many-body systems as quantum channels for transferring information between two distant parties[7].

The Hubbard model with alternating bonds.   One way to achieve localizable entanglement in fermionic systems is to model the interaction between the spins with bonds of alternating strengths $(1 - \delta)$ (weak bond) and $(1 + \delta)$ (strong bond) with $0 \leq \delta \leq 1$. Accordingly, the Fermi–Hubbard model, Eq. (1), transforms onto

$$H = -\sum_{i,\sigma}(1 + (-1)^i\delta)\left(c_{i,\sigma}^\dagger c_{i+1,\sigma} + c_{i+1,\sigma}^\dagger c_{i,\sigma}\right) + U\sum_i n_{i,\uparrow}n_{i,\downarrow}, \tag{15}$$

which is equivalent to the celebrated Su-Schrieffer-Heeger-Hubbard (SSHH) chain. The SSHH model without interaction ($U = 0$) can be used to describe a one-dimensional topological insulator[75] and certain polymers, such as: polyacetylene[76,77]. When the interaction U is present, the SSHH model presents richer topological phases[78], and it has been shown that inspecting the entanglement spectrum of the model reveals the topological phases of
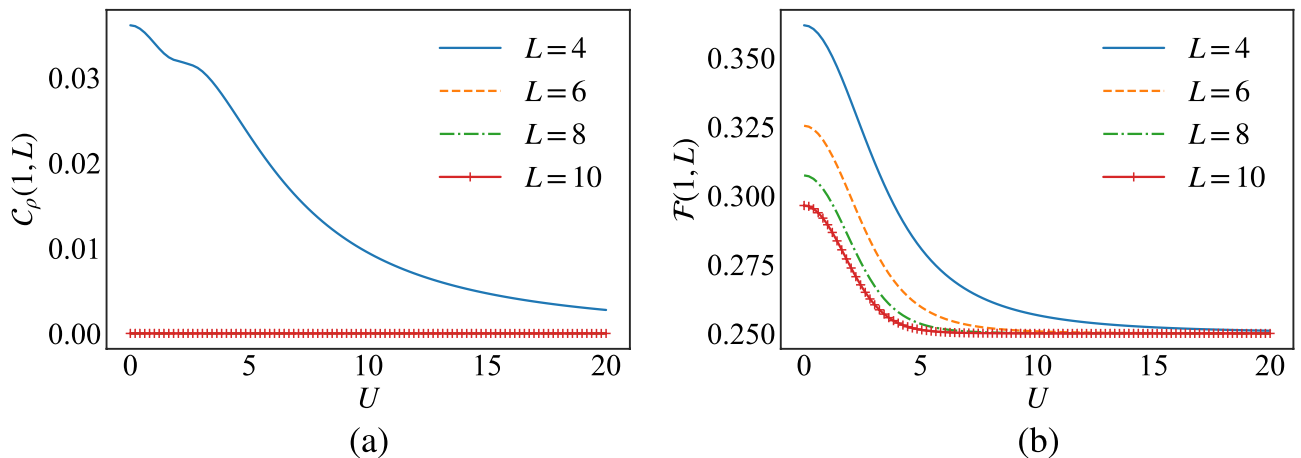
Figure 1. (**a**) The end-to-end concurrence, Eq. (13), and (**b**) the fidelity, Eq. (9), versus U in the Fermi–Hubbard model, Eq. (1), for several chain sizes L.

the SSSH model[79]. Choosing L to be even and $0 \leq \delta \leq 1$ in the Hamiltonian, Eq. (15), ensures that the spins at the end of the chain interact with a weak bond of strength $(1-\delta)$ with their respective neighbors.

The Hubbard model supports a sizable end-to-end entanglement for specific values of the microscopic parameter δ. The end-to-end concurrence, Eq. (13), in the ground state of the Fermi–Hubbard model, Eq. (15), is plotted in Fig. 2a as a function of the parameter δ for various system sizes L and $U = 0$. The numerical data shows the creation of long distance entanglement as the parameter δ is increased, and reaches, asymptotically, the unit value as δ tends to 1. In conjunction with that, the threshold δ_T indicating the birth of long distance entanglement grows with the system size L. This is related essentially to the size effect. Indeed, as the system size increases, the amount of the end-to-end entanglement decreases, and with the increase of δ, this allows to generate new quantum correlations that will be added to the preexisting ones, when $\delta = 0$, which allows thus for the early appearance of the threshold as the system size deceases.

For instance, for $L = 4$ the long distance entanglement appears from $\delta = 0$, because already the end-to-end concurrence associated with the pair $\rho_{1,4}$ in the ground state of the Fermi–Hubbard model Eq. (1) exhibits a non-vanishing value, as sketched in Fig. 1a. In this case, the increase of δ allows for an immediate increase of the long distance entanglement. However, increasing the system size to $L = 6$ for example, it is clear from Fig. 1a that the end-to-end concurrence vanishes for the pair $\rho_{1,6}$, and in this case a threshold δ_T manifests around 0.2 for $L \geq 6$, to create long distance entanglement. (c.f. Fig. 2a)

Nevertheless, a rapid assent to the asymptotic value of long distance entanglement is clear in Fig. 2a as the size of the chain L increases. As a matter of fact, as L grows, the pairwise entanglement at the borders $\rho_{1,2}$ and $\rho_{L-1,L}$ declines[50], and since the role of δ is to locate great amount of entanglement between the end sites (ρ_1 and ρ_L) by excluding entanglement inside the pairs ($\rho_{1,2}$ and $\rho_{L-1,L}$) at the borders, the rate of degradation of the entanglement inside $\rho_{1,2}$ and $\rho_{L-1,L}$ becomes faster as L grows with increasing δ, which accelerate the creation of long distance entanglement between the ends of the chain.

Figure 2b shows the effect of the Coulomb interaction U on the end-to-end concurrence, Eq. (13), of the ground state of the Fermi–Hubbard model, Eq. (15), with respect to the parameter δ, for $L = 10$. When $U = 0$, the long distance entanglement grows slowly but reaches asymptotically the unit value as δ tends to one. However, for non zero values of U, the entanglement grows rapidly up to the asymptotic value of 0.8. Moreover, the threshold δ_T marking the birth of long distance entanglement, diminishes for $U > 0$. This behaviour can be explained by the fact that the state of the pairs at the ends $\rho_{1,L}$ is described by the mixture $\sum_i P_i |\psi\rangle \langle\psi|$ which is generally dominated by the local half filled state (LHFS)[50] associated with the probability P_{LHFS}. For $U = 0$ the LHFS is given by the state $|\psi\rangle_{U=0} = \frac{1}{2}(|\uparrow,\downarrow\rangle + |\downarrow,\uparrow\rangle + |\uparrow\downarrow,0\rangle + |0,\uparrow\downarrow\rangle)$, which indicates the free motion of electrons between the sites. Nevertheless, the increase of δ reduces the effect of the hopping inside the pairs at the borders, which in turn reduces the quantum correlations in the form of entanglement, due to the probability P_{LHFS} becoming insignificant. In contrast, according to the monogamy principle (Ref), the end-to-end entanglement grows since, in this case, P_{LHFS} associated to the maximally entangled pure state ψ_{LHFS} increases and reaches the maximum value 1 at $\delta = 1$, as shown in Fig. 2c. This explains the maximum attainable value 1 of the end-to-end entanglement at $\delta = 1$ when $U = 0$.

Switching on the interaction $U(u/t > 0)$, increases the in-site repulsion interaction which makes the electrons avoid the state of double occupancy. In this case, the local half filled state evolves with δ into the antiferromagnetic state $|\psi\rangle_{U>0} = \frac{1}{\sqrt{2}}(|\uparrow,\downarrow\rangle + |\downarrow,\uparrow\rangle)$ at $\delta = 1$. Simultaneously, P_{LHFS} associated to this state evolves into the maximum unit value at $\delta = 1$. In such circumstances, $\rho_{1,L}$ is well described by a maximally entangled pure state. However, the quantum correlations contained in this state are less than those contained in $|\psi\rangle_{U=0}$, and for this reason the concurrence, Eq. (13), saturates at 0.8 instead of 1 when $U = 0$.

We turn our attention to the behaviour of the fidelity of quantum teleportation when the channel is described by the ground state of the Fermi–Hubbard model, Eq. (15). Figure 3a shows the behavior of the fidelity as a function of δ for different values of the system size L, at $U = 0$. We see that for weak values of δ, the smaller the system size, the faster the fidelity rises up above the classical threshold $\mathscr{F} = \frac{2}{5}$ (dotted line). Nevertheless, as soon as the fidelity rise above the classical threshold, it grows rapidly with δ as the system size increases, reaching the saturation value 0.5 in the limiting case $\delta \to 1$. In the following, we will show how to bypass this saturation value by using the notion of Hubbard projective measurement in the quantum teleportation protocol.
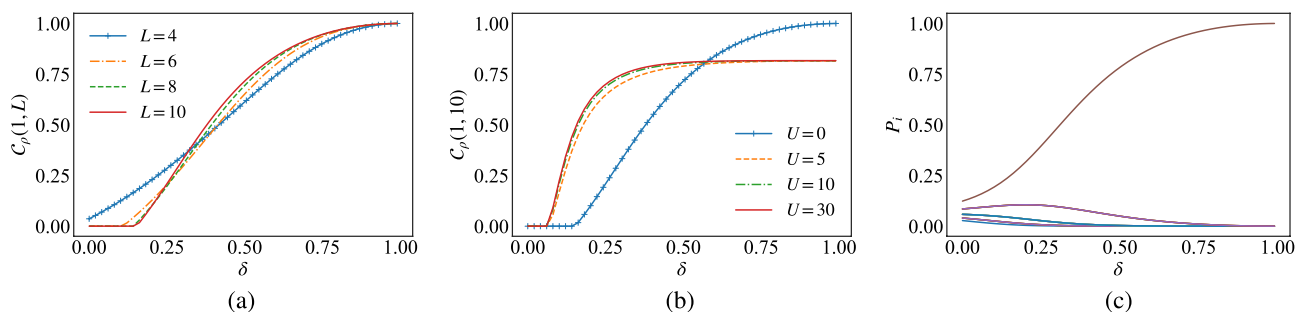
Figure 2. (**a**)+(**b**) The end-to-end concurrence, Eq. (13), with respect to δ for different chain sizes L, and for various values of U with fixed L, respectively. (**c**) Evolution of the occupation probabilities P_i of the local half filled state with respect to δ.
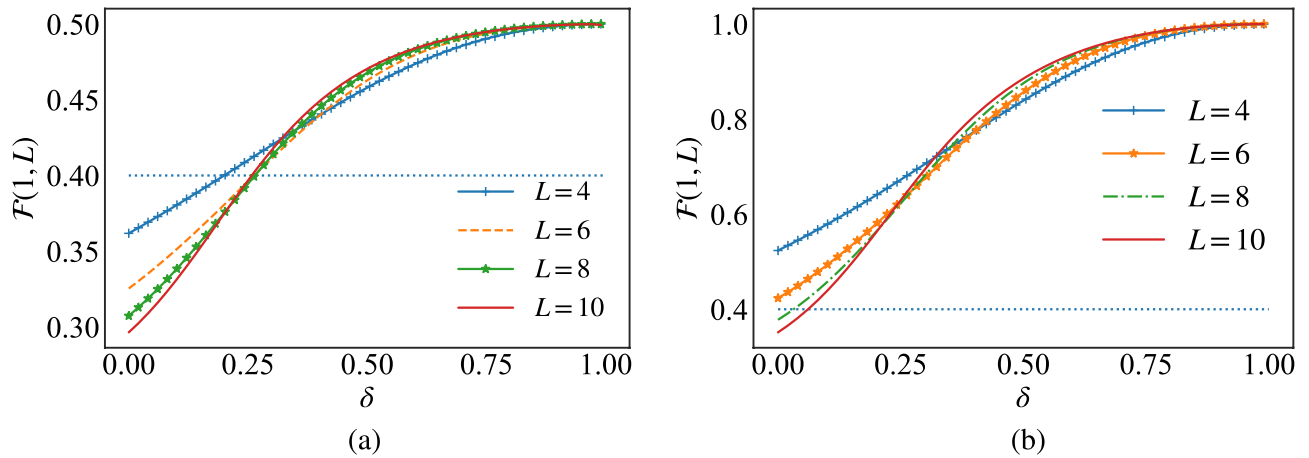
Figure 3. The fidelity, Eq. (9), with respect to δ for several chain sizes. In (**a**) Bell state projection are performed, while (**b**) consists of Hubbard projective measurements.

Teleportation protocol with Hubbard projective measurement. We have demonstrated that the ground state of the Fermi–Hubbard, Eq. (15), with alternating weak and strong bonds allows for efficient quantum teleportation with a fidelity showing quantum advantage. The results found overlap with the data generated for creating long distance entanglement in the ground state of the Heisenberg spin chain, by alternating the interaction J between the sites[7]. However, for the Fermi–Hubbard model a maximally entangled state with concurrence $C(\rho_{1L}) = 1$ seems to be insufficient for teleportation with unit fidelity and only 50% of the information is transferred. Indeed, such a behavior is related to the inappropriate basis choice in the measurement protocol. In the standard quantum teleportation protocol, the four-dimensional maximally entangled Bell state $|\psi^{\dagger}\rangle$, Eq. (8), is employed as the entanglement resource to teleport a four-dimensional quantum state $|\Psi\rangle$, Eq. (6), where the Bell measurement is associated with the set of measurement operators $\{|\psi^{nm}\rangle\langle\psi^{nm}|\}$ such that

$$|\psi^{nm}\rangle = (U^{nm} \otimes I)|\psi^{+}\rangle \tag{16}$$

with $n, m = 0, 1, 2, 3$. In this case, the maximally entangled Bell state projectors

$$E^{nm} = U^{nm}|\psi^{+}\rangle\langle\psi^{+}|(U^{nm})^{\dagger}, \tag{17}$$

are not suitable for the Fermi–Hubbard states (the mixed entangled state resource ρ_{ij}) in the measurement receiver process. This can be clearly seen from the the fully entangled fraction f, Eq. (11), where $f = 1$ only if the state $|\psi^{+}\rangle$ and the entangled quantum state resource are identical, where the quantum state resource χ in (11) represents the density matrix ρ_{ij} associated with two different sites of the Fermi–Hubbard model. Therefore, we propose an adequate projective measurements based on the maximally entangled Hubbard state, i.e. the local half filled state[50]

$$|\psi\rangle_{LHFS} = \frac{1}{2}(|\uparrow, \downarrow\rangle + |\downarrow, \uparrow\rangle + |\uparrow\downarrow, 0\rangle + |0, \uparrow\downarrow\rangle). \tag{18}$$

This allows for the generation of a new framework based on the inherent properties of the Hubbard model, the set of Hubbard projective measurements that are defined by

$$E_{H}^{nm} = U^{nm}|\psi_{LHFS}\rangle\langle\psi_{LHFS}|(U^{nm})^{\dagger}, \tag{19}$$

in such away that the condition $\sum_{nm} Tr[E_{H}^{nm}\rho_{ij}] = 1$ is satisfied and the sixteen generated states $|\psi^{nm}\rangle$, Eq. (16), with $n, m = 0, 1, 2, 3$, are orthonormal and maximally entangled states. This representation is more convenient for quantum teleportation in the Fermi–Hubbard model with unit fidelity. This is confirmed in Fig. 3b, where the end-to-end fidelity rise above the classical threshold (dotted line) quickly and saturates at the unit value as $\delta \to 1$.

Hubbard model with alternating hopping amplitudes. In this part, we discuss another way to create long distance entanglement by modeling the hopping interaction of the Fermi–Hubbard model via alternating hopping amplitudes τ_a and τ_b, as sketched in Fig. 4. In this case the Hamiltonian can be written as:

$$H = -\sum_{i,\sigma} \tau_a \left(c_{2i-1,\sigma}^{\dagger} c_{2i,\sigma} + c_{2i,\sigma}^{\dagger} c_{2i-1,\sigma} \right) + \tau_b \left(c_{2i,\sigma}^{\dagger} c_{2i+1,\sigma} + c_{2i+1,\sigma}^{\dagger} c_{2i,\sigma} \right) + u \sum_{i} n_{i,\uparrow} n_{i,\downarrow}. \tag{20}$$

Figure 5a shows that when $\tau_b < \tau_a$ no end-to-end entanglement is produced and this is related to the fact that the state of the pairs at borders $\rho_{1,2}$ and $\rho_{L-1,L}$ in this case are strongly correlated and there is no entanglement to share between the end sites. Increasing τ_b, the end-to-end entanglement grows rapidly starting from a threshold value that satisfies $\tau_{b_T} \geq \tau_a$, and is dependent on the size of the chain L. This behaviour translates in the fidelity
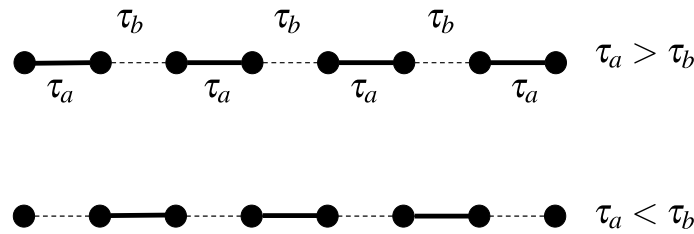
Figure 4. Sketch of the hopping bonds in the Hubbard chain, Eq. (20), with non uniform alternating τ_a and τ_b.
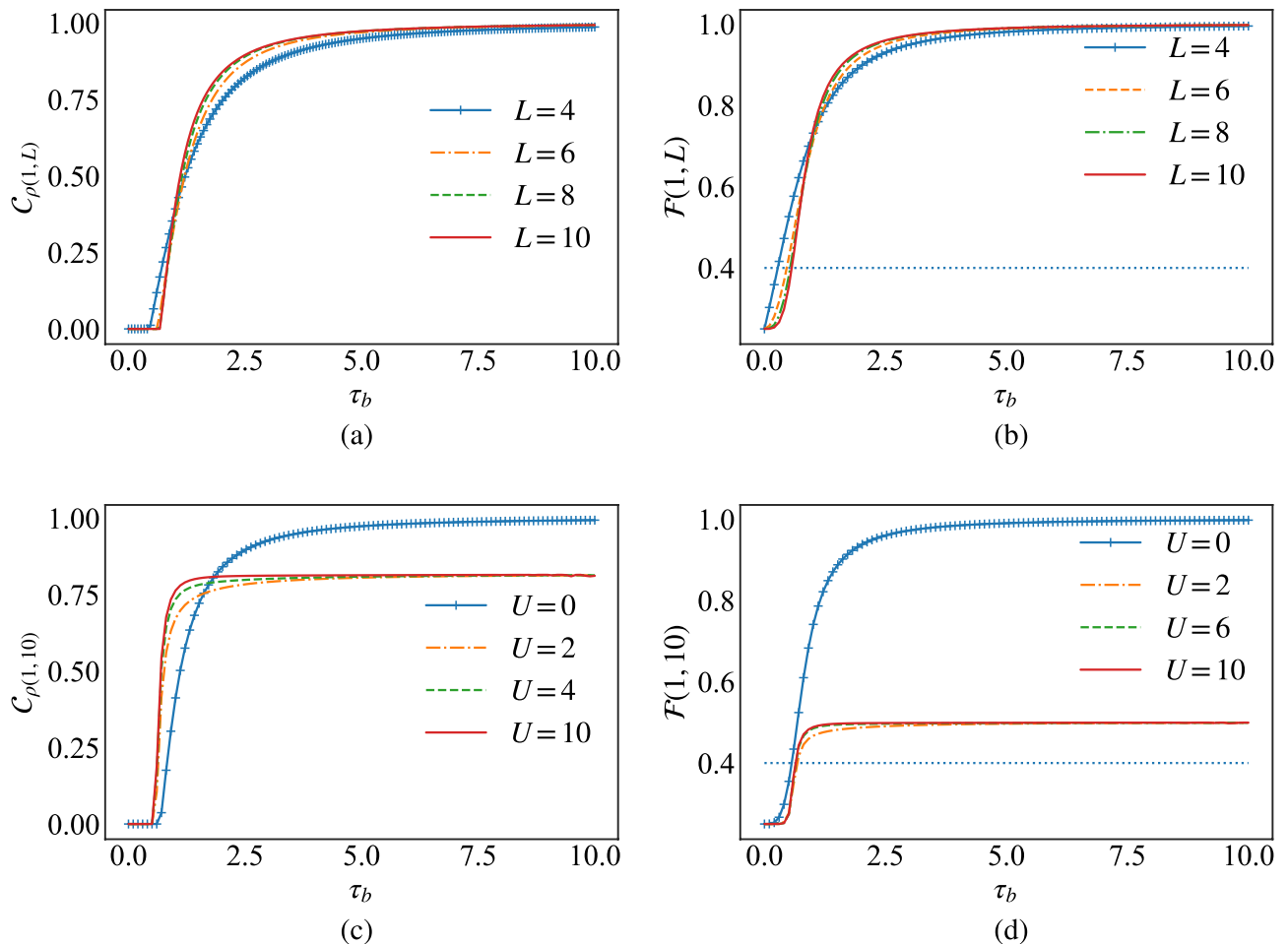
Figure 5. (**a**)+(**b**) The end-to-end concurrence, Eq. (13), and fidelity, Eq. (9), respectively, with respect to τ_b for several chain sizes L. (**c**)+(**d**) The same functions for different values of U and fixed chain length L.

of teleportation which grows more rapidly to 1 while increasing τ_b for smaller chain sizes L, as shown in Fig. 5b. The effect of the Coulomb interaction on the end-to-end entanglement for a chain of $L = 10$ is depicted in Fig. 5c, where we see the threshold value is independent of U when $U > 0$. Additionally, the end-to-end concurrence rise rapidly to 1 for zero Coulomb interaction, while it reaches the asymptotic value of 0.8 for $U > 0$. Here again, the fidelity of teleportation follow the behavior of entanglement shown in Fig. 5d for $L = 10$, where we see that the slight reduction in the amount of the entanglement between the ends of the chain due to the Coulomb interaction, translates into large losses in the fidelity of the quantum teleportation. We note here that the Hubbard projective measurements have been used in the protocol in order to achieve unit fidelity of the quantum teleportation, which in combination with the alternating hopping amplitudes renders the protocol independent of the input state to be teleported (c.f. Figure S2 in the supplementary materials).

Conclusion

In summary, we have examined the ability of the one-dimensional Fermi–Hubbard model to support long distance entanglement in order to exploit its ground state as a channel for quantum teleportation between distant parties. To achieve the goal, we considered the Fermi–Hubbard model with bonds of alternating strengths, and alternating hopping amplitudes. We have established, for both cases, that long distance entanglement can hold with a maximum unit value independently of the system size, only for zero Couloumb interaction. Exploiting the property of long distance entanglement generation in the ground state of the Fermi–Hubbard model, and considering the fact that the quantum states of such model are four dimensional states, we have successfully demonstrated the capability of the one dimensional Fermi–Hubbard chains to operate as quantum channels for four dimensional state teleportation. Finally, we showed the crucial role of the measurement basis in the standard teleportation protocol, where a unit fidelity cannot be attained only by choosing an adequate basis choice based on the inherent properties of the chosen quantum channel, i.e maximally entangled Hubbard states. Our results motivate the investigation of long distance entanglement in the ground state of the Bose-Hubbard model and the Fermi–Bose–Hubbard model in order to inspect the role of symmetry of the ground state on the generation of entanglement, and on the fidelity of information transfer.

Data availability

The datasets generated and analysed during the current study are available from the corresponding author on reasonable request.

References

1. Nielsen, M. & Chuang, I. *Quantum Computation and Quantum Information*, 10th Anniversary Edition. https://doi.org/10.1017/CBO9780511976667 (Cambridge University Press, Cambridge, 2010).
2. Lars, J (2018). *The Second Quantum Revolution: From Entanglement to Quantum Computing and Other Super-Technologies*. https://doi.org/10.1007/978-3-319-98824-5 (Springer, 2018).
3. Bennett, C. H. *et al.* Teleporting an unknown quantum state via dual classical and Einstein–Podolsky–Rosen channels. *Phys. Rev. Lett.* **70**, 1895–1899. https://doi.org/10.1103/PhysRevLett.70.1895 (1993).
4. Bouwmeester, D. *et al.* Experimental quantum teleportation. *Nature* **390**, 575–579 (1997).
5. Boschi, D., Branca, S., De Martini, F., Hardy, L. & Popescu, S. Experimental realization of teleporting an unknown pure quantum state via dual classical and Einstein–Podolsky–Rosen channels. *Phys. Rev. Lett.* **80**, 1121–1125. https://doi.org/10.1103/PhysRevLett.80.1121 (1998).
6. Miranowicz, A. & Tamaki, K. An introduction to quantum teleportation. arXiv:quant-ph/0302114 (2003).
7. Campos Venuti, L., Degli Esposti Boschi, C. & Roncaglia, M. Long-distance entanglement in spin systems. *Phys. Rev. Lett.* **96**, 247206. https://doi.org/10.1103/PhysRevLett.96.247206 (2006).
8. Bose, S. Quantum communication through an unmodulated spin chain. *Phys. Rev. Lett.* **91**, 207901. https://doi.org/10.1103/PhysRevLett.91.207901 (2003).
9. Subrahmanyam, V. Entanglement dynamics and quantum-state transport in spin chains. *Phys. Rev. A* **69**, 034304. https://doi.org/10.1103/PhysRevA.69.034304 (2004).
10. Osborne, T. J. & Linden, N. Propagation of quantum information through a spin system. *Phys. Rev. A* **69**, 052315. https://doi.org/10.1103/PhysRevA.69.052315 (2004).
11. Li, Y., Shi, T., Chen, B., Song, Z. & Sun, C.-P. Quantum-state transmission via a spin ladder as a robust data bus. *Phys. Rev. A* **71**, 022301. https://doi.org/10.1103/PhysRevA.71.022301 (2005).
12. Amico, L., Fazio, R., Osterloh, A. & Vedral, V. Entanglement in many-body systems. *Rev. Mod. Phys.* **80**, 517 (2008).
13. Abaach, S., El Baz, M. & Faqir, M. Pairwise quantum correlations in four-level quantum dot systems. *Phys. Lett. A* **391**, 127140 (2021).
14. Mzaouali, Z. & El Baz, M. Long range quantum coherence, quantum & classical correlations in Heisenberg xx chain. *Phys. A Stat. Mech. Appl.* **518**, 119–130 (2019).
15. Mzaouali, Z., Campbell, S. & El Baz, M. Discrete and generalized phase space techniques in critical quantum spin chains. *Phys. Lett. A* **383**, 125932 (2019).
16. Nikolopoulos, G. & Jex, I. *Quantum State Transfer and Network Engineering. Quantum Science and Technology* (Springer, Berlin, 2013).
17. Apollaro, T. J., Lorenzo, S. & Plastina, F. Transport of quantum correlations across a spin chain. *Int. J. Mod. Phys. B* **27**, 1345035 (2013).
18. Lorenzo, S., Apollaro, T. J. G., Sindona, A. & Plastina, F. Quantum-state transfer via resonant tunneling through local-field-induced barriers. *Phys. Rev. A* **87**, 042313. https://doi.org/10.1103/PhysRevA.87.042313 (2013).
19. Apollaro, T. J. G., Lorenzo, S., Plastina, F., Consiglio, M. & Życzkowski, K. Quantum transfer of interacting qubits. *New J. Phys.* **24**, 083025. https://doi.org/10.1088/1367-2630/ac86e7 (2022).
20. Yousefjani, R. & Bayat, A. Parallel entangling gate operations and two-way quantum communication in spin chains. *Quantum* **5**, 460 (2021).
21. Hermes, S., Apollaro, T. J., Paganelli, S. & Macrì, T. Dimensionality-enhanced quantum state transfer in long-range-interacting spin systems. *Phys. Rev. A* **101**, 053607 (2020).
22. Pouyandeh, S. & Shahbazi, F. Quantum state transfer in xxz spin chains: A measurement induced transport method. *Int. J. Quantum Inf.* **13**, 1550030 (2015).
23. Lorenzo, S., Apollaro, T., Paganelli, S., Palma, G. & Plastina, F. Transfer of arbitrary two-qubit states via a spin chain. *Phys. Rev. A* **91**, 042321 (2015).
24. Yang, Z., Gao, M. & Qin, W. Transfer of high-dimensional quantum state through an xxz-Heisenberg quantum spin chain. *Int. J. Mod. Phys. B* **29**, 1550207 (2015).
25. Bayat, A. Arbitrary perfect state transfer in d-level spin chains. *Phys. Rev. A* **89**, 062302 (2014).
26. Apollaro, T. *et al.* Many-qubit quantum state transfer via spin chains. *Phys. Scr.* **2015**, 014036 (2015).
27. Osborne, T. J. & Nielsen, M. A. Entanglement in a simple quantum phase transition. *Phys. Rev. A* **66**, 032110. https://doi.org/10.1103/PhysRevA.66.032110 (2002).
28. Osterloh, A., Amico, L., Falci, G. & Fazio, R. Scaling of entanglement close to a quantum phase transition. *Nature* **416**, 608–610. https://doi.org/10.1038/416608a (2002).

29. Jin, B.-Q. & Korepin, V. E. Localizable entanglement in antiferromagnetic spin chains. *Phys. Rev. A* **69**, 062314. https://doi.org/10.1103/PhysRevA.69.062314 (2004).
30. Campos Venuti, L., Giampaolo, S. M., Illuminati, F. & Zanardi, P. Long-distance entanglement and quantum teleportation in *xx* spin chains. *Phys. Rev. A* **76**, 052328. https://doi.org/10.1103/PhysRevA.76.052328 (2007).
31. Xiao-Qiang, X. & Wu-Ming, L. Generation of long-distance entanglement in spin system. *Chin. Phys. Lett.* **25**, 2346–2349. https://doi.org/10.1088/0256-307x/25/7/005 (2008).
32. Giampaolo, S. M. & Illuminati, F. Long-distance entanglement in many-body atomic and optical systems. *New J. Phys.* **12**, 025019. https://doi.org/10.1088/1367-2630/12/2/025019 (2010).
33. Dell'Anna, L. Long-distance entanglement in Motzkin and Fredkin spin chains. *SciPost Phys.* **7**, 053. https://doi.org/10.21468/SciPostPhys.7.4.053 (2019).
34. Hu, L.-Z., Xu, Y.-L., Zhang, P.-P., Yan, S.-W. & Kong, X.-M. Long-distance entanglement in antiferromagnetic xxz spin chain with alternating interactions. *Phys. A Stat. Mech. Appl.*https://doi.org/10.1016/j.physa.2022.128170 *(2022)*.
35. Cui, J. & Mintert, F. Robust control of long-distance entanglement in disordered spin chains. *New J. Phys.* **17**, 093014. https://doi.org/10.1088/1367-2630/17/9/093014 (2015).
36. Rafiee, M. Measurement enhances long-distance entanglement generation in spin chains with dissipative processes. *Eur. Phys. J. D*https://doi.org/10.1140/epjd/e2018-90297-1 *(2018)*.
37. Sahling, S. *et al.* Experimental realization of long-distance entanglement between spins in antiferromagnetic quantum spin chains. *Nat. Phys.* **11**, 255–260 (2015).
38. Campos Venuti, L., Degli Esposti Boschi, C. & Roncaglia, M. Qubit teleportation and transfer across antiferromagnetic spin chains. *Phys. Rev. Lett.* **99**, 060401. https://doi.org/10.1103/PhysRevLett.99.060401 (2007).
39. Gröblacher, S., Jennewein, T., Vaziri, A., Weihs, G. & Zeilinger, A. Experimental quantum cryptography with qutrits. *New J. Phys.* **8**, 75–75. https://doi.org/10.1088/1367-2630/8/5/075 (2006).
40. Mafu, M. *et al.* Higher-dimensional orbital-angular-momentum-based quantum key distribution with mutually unbiased bases. *Phys. Rev. A* **88**, 032305. https://doi.org/10.1103/PhysRevA.88.032305 (2013).
41. Cerf, N. J., Bourennane, M., Karlsson, A. & Gisin, N. Security of quantum key distribution using *d*-level systems. *Phys. Rev. Lett.* **88**, 127902. https://doi.org/10.1103/PhysRevLett.88.127902 (2002).
42. Huber, M. & Pawłowski, M. Weak randomness in device-independent quantum key distribution and the advantage of using high-dimensional entanglement. *Phys. Rev. A* **88**, 032309. https://doi.org/10.1103/PhysRevA.88.032309 (2013).
43. Wang, X.-L. *et al.* Quantum teleportation of multiple degrees of freedom of a single photon. *Nature* **518**, 516–519 (2015).
44. Zhou, L. & Sheng, Y.-B. Complete logic bell-state analysis assisted with photonic faraday rotation. *Phys. Rev. A* **92**, 042314. https://doi.org/10.1103/PhysRevA.92.042314 (2015).
45. Sheng, Y.-B., Deng, F.-G. & Long, G. L. Complete hyperentangled-bell-state analysis for quantum communication. *Phys. Rev. A* **82**, 032318. https://doi.org/10.1103/PhysRevA.82.032318 (2010).
46. Qiao, H. *et al.* Conditional teleportation of quantum-dot spin states. *Nat. Commun.* **11**, 1–9 (2020).
47. Luo, Y.-H. *et al.* Quantum teleportation in high dimensions. *Phys. Rev. Lett.* **123**, 070505. https://doi.org/10.1103/PhysRevLett.123.070505 (2019).
48. El Kirdi, M., Slaoui, A., Ikken, N., Daoud, M. & Ahl Laamara, R. Controlled quantum teleportation between discrete and continuous physical systems. *Phys. Scr.* **98**, 025101 (2022).
49. Nichol, J. M. Quantum-dot spin chains. In *Entanglement in Spin Chains* (eds Bayat, A. *et al.*) 505–538 (Springer, Berlin, 2022).
50. Abaach, S., Faqir, M. & El Baz, M. Long-range entanglement in quantum dots with Fermi–Hubbard physics. *Phys. Rev. A* **106**, 022421. https://doi.org/10.1103/PhysRevA.106.022421 (2022).
51. Hubbard, J. Electron correlations in narrow energy bands. *Proc. R. Soc.* **276**, 238. https://doi.org/10.1098/rspa.1963.0204 (1963).
52. Hensgens, T. *et al.* Quantum simulation of a Fermi–Hubbard model using a semiconductor quantum dot array. *Nature* **548**, 70–73. https://doi.org/10.1038/nature23022 (2017).
53. Essler, F. H., Frahm, H., Göhmann, F., Klümper, A. & Korepin, V. E. *The One-dimensional Hubbard Model* (Cambridge University Press, Cambridge, 2005).
54. Anfossi, A., Giorda, P. & Montorsi, A. Entanglement in extended Hubbard models and quantum phase transitions. *Phys. Rev. B* **75**, 165106 (2007).
55. Gu, S.-J., Deng, S.-S., Li, Y.-Q. & Lin, H.-Q. Entanglement and quantum phase transition in the extended Hubbard model. *Phys. Rev. Lett.* **93**, 086402 (2004).
56. Kleftogiannis, I., Amanatidis, I. & Popkov, V. Exact results for the entanglement in 1d Hubbard models with spatial constraints. *J. Stat. Mech. Theory Exp.* **2019**, 063102 (2019).
57. Canella, G. A. & França, V. V. Superfluid-insulator transition unambiguously detected by entanglement in one-dimensional disordered superfluids. *Sci. Rep.* **9**, 1–6 (2019).
58. Harir, S., Zouhair, A., Boulahia, Z., Kazaz, M. & Boughaleb, Y. Quantum entanglement in ground state of extended Hubbard model. *Int. J. Theor. Phys.* **58**, 3149–3157 (2019).
59. Spalding, J., Tsai, S.-W. & Campbell, D. K. Critical entanglement for the half-filled extended Hubbard model. *Phys. Rev. B* **99**, 195445. https://doi.org/10.1103/PhysRevB.99.195445 (2019).
60. Zawadzki, K., Serra, R. M. & D'Amico, I. Work-distribution quantumness and irreversibility when crossing a quantum phase transition in finite time. *Phys. Rev. Res.* **2**, 033167 (2020).
61. Tarruell, L. & Sanchez-Palencia, L. Quantum simulation of the Hubbard model with ultracold fermions in optical lattices. *C. R. Phys.* **19**, 365–393. https://doi.org/10.1016/j.crhy.2018.10.013 (2018) (**Quantum simulation / Simulation quantique.**).
62. Bowen, G. & Bose, S. Teleportation as a depolarizing quantum channel, relative entropy, and classical capacity. *Phys. Rev. Lett.* **87**, 267901 (2001).
63. Jozsa, R. Fidelity for mixed quantum states. *J. Mod. Opt.* **41**, 2315–2323. https://doi.org/10.1080/09500349414552171 (1994).
64. Horodecki, M., Horodecki, P. & Horodecki, R. General teleportation channel, singlet fraction, and quasidistillation. *Phys. Rev. A* **60**, 1888–1898. https://doi.org/10.1103/PhysRevA.60.1888 (1999).
65. Bennett, C. H., DiVincenzo, D. P., Smolin, J. A. & Wootters, W. K. Mixed-state entanglement and quantum error correction. *Phys. Rev. A* **54**, 3824–3851. https://doi.org/10.1103/PhysRevA.54.3824 (1996).
66. Albeverio, S., Fei, S.-M. & Yang, W.-L. Optimal teleportation based on bell measurements. *Phys. Rev. A* **66**, 012301. https://doi.org/10.1103/PhysRevA.66.012301 (2002).
67. Horodecki, R., Horodecki, P., Horodecki, M. & Horodecki, K. Quantum entanglement. *Rev. Mod. Phys.* **81**, 865–942. https://doi.org/10.1103/RevModPhys.81.865 (2009).
68. Ou, Y.-C., Fan, H. & Fei, S.-M. Proper monogamy inequality for arbitrary pure quantum states. *Phys. Rev. A* **78**, 012311. https://doi.org/10.1103/PhysRevA.78.012311 (2008).
69. Li, M., Fei, S.-M. & Wang, Z.-X. A lower bound of concurrence for multipartite quantum states. *J. Phys. A: Math. Theor.* **42**, 145303. https://doi.org/10.1088/1751-8113/42/14/145303 (2009).
70. Zhu, X.-N., Li, M. & Fei, S.-M. Lower bounds of concurrence for multipartite states. In *AIP Conference Proceedings*, Vol. 1424. https://doi.org/10.1063/1.3688955 (2012).
71. Weinberg, P. & Bukov, M. Quspin: A python package for dynamics and exact diagonalisation of quantum many body systems part i: Spin chains. *SciPost Phys.* **2**, 1. https://doi.org/10.21468/scipostphys.2.1.003 (2017).

72. Johansson, J., Nation, P. & Nori, F. Qutip 2: A python framework for the dynamics of open quantum systems. Part II: Bosons, fermions and higher spins. *Comput. Phys. Commun.* **184**, 1234–1240. https://doi.org/10.1016/j.cpc.2012.11.019 (2013).
73. Johansson, J., Nation, P. & Nori, F. Qutip 2: A python framework for the dynamics of open quantum systems. *Comput. Phys. Commun.* **184**, 1234–1240. https://doi.org/10.1016/j.cpc.2012.11.019 (2013).
74. Johansson, J., Nation, P. & Nori, F. Qutip: An open-source python framework for the dynamics of open quantum systems. *Comput. Phys. Commun.* **183**, 1760–1772. https://doi.org/10.1016/j.cpc.2012.02.021 (2012).
75. Guo, H. & Shen, S.-Q. Topological phase in a one-dimensional interacting fermion system. *Phys. Rev. B* **84**, 195107. https://doi.org/10.1103/PhysRevB.84.195107 (2011).
76. Su, W. P., Schrieffer, J. R. & Heeger, A. J. Solitons in polyacetylene. *Phys. Rev. Lett.* **42**, 1698–1701. https://doi.org/10.1103/PhysRevLett.42.1698 (1979).
77. Heeger, A. J., Kivelson, S., Schrieffer, J. R. & Su, W. P. Solitons in conducting polymers. *Rev. Mod. Phys.* **60**, 781–850. https://doi.org/10.1103/RevModPhys.60.781 (1988).
78. Wang, D., Xu, S., Wang, Y. & Wu, C. Detecting edge degeneracy in interacting topological insulators through entanglement entropy. *Phys. Rev. B* **91**, 115118. https://doi.org/10.1103/PhysRevB.91.115118 (2015).
79. Ye, B.-T., Mu, L.-Z. & Fan, H. Entanglement spectrum of Su–Schrieffer–Heeger–Hubbard model. *Phys. Rev. B* **94**, 165167. https://doi.org/10.1103/PhysRevB.94.165167 (2016).

Acknowledgements

Author contributions

The authors confirm contribution to the paper as follows: study conception and data collection: S.A., Z.M.; analysis and interpretation of results: S.A., Z.M., M.E.B.; draft manuscript preparation: S.A., Z.M., M.E.B. All authors reviewed the results and approved the final version of the manuscript.

Competing interests

The authors declare no competing interests.

Additional information

Supplementary Information The online version contains supplementary material available at https://doi.org/10.1038/s41598-023-28180-4.

Correspondence and requests for materials should be addressed to Z.M.

Reprints and permissions information is available at www.nature.com/reprints.

Publisher's note Springer Nature remains neutral with regard to jurisdictional claims in published maps and institutional affiliations.